Characterization of the mechanism of action, pharmacodynamics and preclinical safety of ADCT-402, a pyrrolobenzodiazepine (PBD) dimer-containing antibody-drug conjugate (ADC) targeting CD19-expressing hematological malignancies

no. 51

Francesca Zammarchi[1], Simon Corbett[3], Karin Havenith[1], Narinder Janghra[3], Konstantinos Kiakos[3], Teresa Marafioti[3], David G Williams[2], Simon Chivers[1], Phil W Howard[2], John A. Hartley[2,3], Patrick H. van Berkel[1]

[1] ADC Therapeutics SA, Epalinges, Switzerland, [2] Spirogen, Medimmune, London, United Kingdom; [3] University College London, London, United Kingdom

Introduction

1. Human CD19 antigen is a 95 kilodalton type I membrane glycoprotein belonging to the immunoglobulin superfamily (Figure 1) [1]. In normal human tissue, expression of CD19 is limited to the various stages of B-cell development and differentiation (except plasma cells) and its expression is maintained on the majority of B-cell malignancies, including B-cell leukemia and non-Hodgkin lymphomas (NHL) of B-cell origin. CD19 has rapid internalization kinetics and it is not shed into the circulation [2, 3].

Figure 1: Structure of CD19.

2. ADCT-402 is an ADC composed of a humanized antibody, directed against human CD19, stochastically conjugated to the highly cytotoxic PBD-based linker-drug tesirine [4] (drug-antibody ratio of 2.3) (Figure 2).

Figure 2: ADCT-402.

3. ADCT-402 has potent and targeted cytotoxicity against a panel of human lymphoma and leukemia cell lines *in vitro* [5].
4. *In vivo*, ADCT-402 demonstrates dose-dependent antitumor activity against Burkitt's lymphoma and leukemia xenograft models. Moreover, ADCT-402 is markedly superior to maytansinoid- and auristatin-based CD19-targeting ADCs in the Ramos xenograft model [5].
5. In a rat toxicology study, a single dose of ADCT-402 at 2 mg/kg is well tolerated with a favourable PK profile and excellent stability *in vivo* [5].

Aim of this study

To further define the mechanism of action of ADCT-402 and validate its pharmacology and pre-clinical safety for clinical development.

Material & Methods

- Binding and internalization were visualized by standard immunofluorescence techniques.
- The single cell gel electrophoresis (Comet) assay was carried out to quantify the amount of DNA interstrand cross-links (ICLs). The mean reduction in the product of the tail length and the fraction of total DNA in the tail, i.e. the Olive Tails Moment (OTM) in irradiated cells was measured.
- *In vivo*, ADCT-402 or a non-targeted ADC was administered intravenously (i.v.) as a single dose to SCID mice containing subcutaneously implanted Ramos xenografts.
- For PK analysis, quantitation of total (unconjugated and conjugated) and PBD-conjugated antibody were determined by ECLIA using a biotinylated mouse anti-idiotype antibody and a biotinylated anti-PBD mouse monoclonal antibody as a capture, respectively. For both assays, a sulfo-tag labeled mouse anti-idiotype antibody was used for detection. The determination of free PBD dimer SG3199 was performed by LC-MC/MS.
- Immunohistochemistry (IHC) analysis on formalin fixed paraffin embedded (FFPE) tumors was performed using mouse anti-human CD19, clone BT51E (Leica-CD19-163) and rabbit phospho-histone H2A.X (Ser 139) (Cell Signaling 9177) antibodies.

Results

Table 1: CD19 expression in matched NHL clinical samples.

NHL subtype	Case # Primary (P)/ Relapsed (R)	Biopsy type	Time between biopsy (months)	CD19 intensity	CD19 heterogeneity
DLBCL	1P	BM	8	2	+
	1R	BM		3	+
	2P	LN	20	3	+
	2R	mesenteric mass		3	+
	3P	testis	12	3	+
	3R	penile mass		3	+
	4P	LN	14	3	+
	4R	LN		3	+
	5P	BM	8	2	+
	5R	LN		3	+
MCL	6P	salivary gland	20	3	+
	6R	submandibular		3	+
	7P	BM	11	3	+
	7R	LN		3	+
	8P	LN	15	3	+
	8R	LN		3	+
	9P	gastrointestinal	8	3	+
	9R	duodenal bulb		3	+
FL	10P	LN	27	3	+
	10R	LN		3	+
	11P	LN	26	3	+
	11R	LN		3	+
CLL	12P	BM	20	3	+
	12R	BM		2	+

CD19 expression is maintained in matched samples (initial diagnosis and relapsed/refractory) from a panel of NHL patients. DLBCL, diffuse large B-cell lymphoma; MCL, mantle cell lymphoma; FL, follicular lymphoma; CLL, chronic lymphocytic leukaemia; BM, bone marrow; LN, lymph node. Intensity of CD19 staining: 0 : negative; 1 :weak; 2 : moderate staining; 3 : strong staining. Heterogeneity of CD19 staining: + > 80% tumour cells are CD19-positive; - > 80% tumour cells are CD19-negative.

Figure 3: Internalization kinetic.

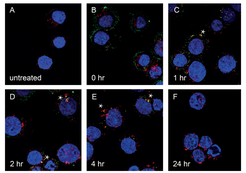

Confocal microscopy images of Ramos cells treated with 2 µg/ml ADCT-402 and stained for nuclei (blue), LAMP-1 (red) and human IgG antibody (green). A. Untreated cells, B. Immediately following exposure to ADCT-402, C. 1 hour post-incubation, D. 2 hours post-incubation, E. 4 hours post-incubation, F. 24 hours post-incubation. Co-staining between LAMP-1 and IgG is observed as yellow and it is indicated by asterisks. hr, hour.

Figure 4: Time course of DNA ICL.

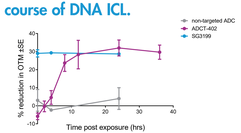

Time course of DNA interstrand cross-link (ICL) formation in Ramos cells following a 2-hour treatment with ADCT-402 (40 pM), the PBD dimer SG3199 (10 pM) or a non-targeted ADC (40 pM). Cells were treated for 2 hours, followed by a drug-free incubation for the indicated post-treatment time. Results are presented as mean % decrease in OTM ± SEM (n=3) relative to irradiated, untreated cells. For ADCT-402, the peak of cross-links occurred between 8 - 12 hours and persisted for up to 36 hours post-treatment.

Figure 5: Pharmacodynamic assays in Ramos xenograft study.

A

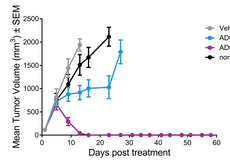

A. ADCT-402 was administered intravenously (i.v.) as a single dose at 0.3 or 1 mg/kg to treatment groups of 7 mice on day 1. An isotype control, non-targeted-ADC (administered as single dose at 1 mg/kg) and a vehicle (PBS) treated group served as controls.

B

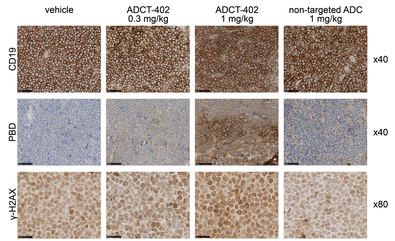

B. Representative scans of FFPE Ramos tumor sections, obtained 24 hours after mice treatment (n=3) with single doses of vehicle, 1 mg/kg non-targeted ADC and 0.3 or 1 mg/kg ADCT-402, stained with an anti-CD19 antibody (top panel), anti-PBD linker antibody (mid panel) and anti-γ-H2AX antibody (bottom panel). Magnification is 40× in top and middle panel images and 80× in bottom panel.

C

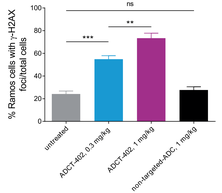

C. Quantification of γ-H2AX foci in tumor sections depicted in B, bottom panel. Four random areas were selected in each tumor block from each mouse (n=3); nuclei with 1 or more γ-H2AX foci were counted. Data are expressed as percentage of total nuclei within the selected area. Bars represent mean ±SEM. ** p≤0.01; ***≤0.001; ns, not significant.

D

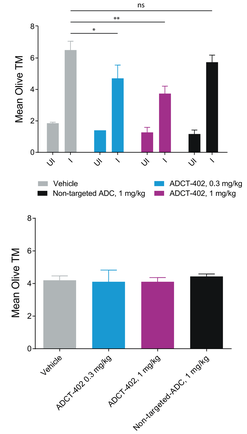

D. Quantification of DNA ICLs. Mean olive tail moment (OTM) in unirradiated (UI) and irradiated (I) tumor cell suspension (upper panel) and irradiated peripheral blood mononuclear cells (PBMCs) (lower panel) taken from Ramos xenografts 24 hours after treatment with single doses of the indicated compounds. *, p ≤ 0.05; ** p≤ 0.01; *** p ≤ 0.001; ns, not significant.

Figure 6: PK analysis in cynomolgus monkey.

A

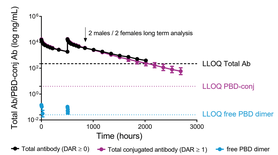

B

Dose day	Cmax	Tmax	Clast	Tlast	T1/2	
	ng/mL	hours	ng/mL	hours	hours	days
1	15750	0.855	1901	504	340	14.1
22	17420	0.672	5502	168	330	13.7

A. Quantitation of total antibody, PBD-conjugated antibody and free PBD dimer in cynomolgus monkey serum after administration of 0.6 mg/kg ADCT-402 on days 1 and 22. The graph show the mean ± SEM (n = 10). **B.** Total antibody PK parameters according to a non-compartimental PK analysis (NCA).

Conclusions

1. CD19 high and homogeneous expression is maintained in a panel of matched NHL samples taken at initial diagnosis and at relapse/refractory, confirming CD19 excellent tumor expression profile for an ADC target.
2. ADCT-402 was specifically bound, internalized and trafficked to the lysosomes in CD19-positive Ramos cells. Co-localization with lysosomes was observed within 1 hour, while by 24 hours no IgG staining was observed, suggesting complete lysosomal degradation of ADCT-402.
3. *In vitro*, ADCT-402 specifically induced DNA ICLs in CD19-positive Ramos cells after a 2-hour exposure, which persisted for at least 36 hours *in vitro*. No cross-links were detected with a control, non-targeted ADC.
4. *In vivo*, single doses of ADCT-402 resulted in specific, potent and dose-dependent anti-tumor activity in the Ramos xenograft model. DNA ICLs were readily measured in tumors by 24 hours from administration of ADCT-402, while matched PBMCs showed no evidence of DNA ICLs. At the same time point, detection of phospho-H2AX immunostaining indicated a DNA-damage response was initiated.
5. ADCT-402 was stable and clinically well tolerated in a repeat dose cynomolgus monkey study at 0.6 mg/kg with an acceptable off-target safety profile. The PK of the ADC, with super-imposable total Ab and PBD-conjugated Ab profiles, was consistent with normal antibody clearance with a half-life of about 14 days.
6. Together, these data further define the *in vitro* and *in vivo* mechanism of action and pre-clinical safety of ADCT-402 and provide relevant pharmacodynamic assays to guide the clinical development of this promising ADC in B-cell malignancies.
7. ADCT-402 is being tested in phase 1 trials recruiting patients with relapsed/refractory B-NHL (*NCT02669017*) and relapsed/refractory acute lymphoblastic leukemia (*NCT02669264*).

Acknowledgements

In vivo experiments: Charles River Discovery Research Services.

References

1. Wang, K., G. Wei, and D. Liu, CD19: a biomarker for B cell development, lymphoma diagnosis and therapy. Exp Hematol Oncol, 2012. 1(1): p. 36.
2. Gerber, H.P., et al., Potent antitumor activity of the anti-CD19 auristatin antibody drug conjugate hBU12-vcMMAE against rituximab-sensitive and -resistant lymphomas. Blood, 2009. 113(18): p. 4352-61.
3. Blanc, V., et al., SAR3419: an anti-CD19-Maytansinoid Immunoconjugate for the treatment of B-cell malignancies. Clin Cancer Res, 2011. 17(20): p. 6448-58.
4. Tiberghien, A.C., et al., Design and Synthesis of Tesirine, a Clinical Antibody-Drug Conjugate Pyrrolobenzodiazepine Dimer Payload. ACS Med Chem Lett, 2016. 7(11): p. 983-987.
5. Zammarchi, F., et al., Pre-clinical Development of ADCT-402, a Novel Pyrrolobenzodiazepine (PBD)-Based Antibody Drug Conjugate (ADC) Targeting CD19-Expressing B-cell Malignancies. Blood, 2015. 126(23).